Received: 16 March 2022 | Revised: 3 January 2023 | Accepted: 30 January 2023

DOI: 10.1111/gbi.12549

ORIGINAL ARTICLE

gebiology WILEY

# A carbonate corrosion experiment at a marine methane seep: The role of aerobic methanotrophic bacteria

Alexmar Cordova-Gonzalez[1] | Daniel Birgel[1] | Max Wisshak[2] | Tim Urich[3] | Florian Brinkmann[4] | Yann Marcon[4] | Gerhard Bohrmann[4] | Jörn Peckmann[1]

[1]Centrum für Erdsystemforschung und Nachhaltigkeit, Universität Hamburg, Institut für Geologie, Hamburg, Germany

[2]Senckenberg am Meer, Abteilung Meeresforschung, Wilhelmshaven, Germany

[3]Center for Functional Genomics of Microbes, University of Greifswald, Institut für Mikrobiologie, Greifswald, Germany

[4]MARUM – Zentrum für Marine Umweltwissenschaften und Fachbereich Geowissenschaften, Universität Bremen, Bremen, Germany

**Correspondence**
Jörn Peckmann, Institut für Geologie, Centrum für Erdsystemforschung und Nachhaltigkeit, Universität Hamburg, 20146 Hamburg, Germany.
Email: joern.peckmann@uni-hamburg.de

**Funding information**
Deutscher Akademischer Austauschdienst

## Abstract

Methane seeps are typified by the formation of authigenic carbonates, many of which exhibit corrosion surfaces and secondary porosity believed to be caused by microbial carbonate dissolution. Aerobic methane oxidation and sulfur oxidation are two processes capable of inducing carbonate corrosion at methane seeps. Although the potential of aerobic methanotrophy to dissolve carbonate was confirmed in laboratory experiments, this process has not been studied in the environment to date. Here, we report on a carbonate corrosion experiment carried out in the REGAB Pockmark, Gabon-Congo-Angola passive margin, in which marble cubes were deployed for 2.5 years at two sites (CAB-B and CAB-C) with apparent active methane seepage and one site (CAB-D) without methane seepage. Marble cubes exposed to active seepage (experiment CAB-C) were found to be affected by a new type of microbioerosion. Based on 16*S rRNA* gene analysis, the biofilms adhering to the bioeroded marble mostly consisted of aerobic methanotrophic bacteria, predominantly belonging to the uncultured Hyd24-01 clade. The presence of abundant $^{13}$C-depleted lipid biomarkers including fatty acids (*n*-$C_{16:1\omega8c}$, *n*-$C_{18:1\omega8c}$, *n*-$C_{16:1\omega5t}$), various 4-mono- and 4,4-dimethyl sterols, and diplopterol agrees with the dominance of aerobic methanotrophs in the CAB-C biofilms. Among the lipids of aerobic methanotrophs, the uncommon 4α-methylcholest-8(14)-en-3β,25-diol is interpreted to be a specific biomarker for the Hyd24-01 clade. The combination of textural, genetic, and organic geochemical evidence suggests that aerobic methanotrophs are the main drivers of carbonate dissolution observed in the CAB-C experiment at the REGAB pockmark.

**KEYWORDS**
carbonate, corrosion, lipid biomarker, methane seep, methanotrophic bacteria, microbioerosion

## 1 | INTRODUCTION

The dynamics of methane seeps have been studied in great detail since this carbon pool may play an important role in global climate change (Kennett et al., 2003) and potentially as energy source (Sloan, 2003). Methane seeps occur along passive and active continental margins, associated with geological features, as for example, gas hydrates, pockmarks, and mud volcanoes (Suess, 2014). It has been shown that many seeps are related to gas hydrate dynamics (Elvert et al., 1999; Suess et al., 1999). The stability of gas hydrate depends on the conditions at the seafloor and in the subsurface, such as temperature, pressure, and the availability of water and gas, predominantly methane (Bohrmann & Torres, 2006). Whether gas hydrate stability and dissociation is controlled by climate change, and how relevant it is for the overall methane seepage dynamics (Kennett et al., 2003) and methane export to the water column and atmosphere, is still a matter of debate (Ruppel & Kessler, 2016). In any case, methane seeps are active over long time periods and are further characterized by the formation of authigenic methane-derived carbonate (e.g., Bohrmann et al., 1998; Greinert et al., 2013; Peckmann et al., 2001), commonly precipitating in anoxic sediments affected by seepage. Seep carbonate is the result of an increase in alkalinity induced by the anaerobic oxidation of methane (AOM; Peckmann & Thiel, 2004), a process mediated by a consortium of methane-oxidizing archaea and sulfate-reducing bacteria (Boetius et al., 2000). Seep carbonates have a global distribution, including numerous modern and ancient deposits (Campbell, 2006 for a review). Although AOM is favoring carbonate precipitation, many seep carbonates exhibit corrosion surfaces and secondary porosity, likely caused by microbially induced carbonate dissolution (e.g., Birgel, Peckmann, et al., 2006; Campbell et al., 2002; Crémière et al., 2012; Himmler et al., 2011; Matsumoto, 1990; Natalicchio et al., 2015).

Carbonate dissolution in the marine realm has received much attention because it is a key process in global carbon cycling (Naviaux et al., 2019; Subhas et al., 2017). However, the role of microbes in carbonate dissolution has received little attention to date (Krause et al., 2014). The two biological processes that have been put forward to induce carbonate corrosion at seeps are aerobic methane oxidation (Cai et al., 2006; Crémière et al., 2012; Himmler et al., 2011; Matsumoto, 1990; Natalicchio et al., 2015) and hydrogen sulfide oxidation (Crémière et al., 2012; Leprich et al., 2021). Both processes can locally lower pH, resulting in carbonate dissolution (Crémière et al., 2012). In particular, aerobic methane oxidation leads to the production of carbon dioxide, with a subsequent increase of $pCO_2$, favoring the dissolution of carbonate (Equation 1; Aloisi et al., 2000). The influence of aerobic methanotrophy on carbonate dissolution has been confirmed in closed-system experiments with the Type II methanotrophic bacterial strain *Methylosinus trichosporium* OB3b, demonstrating that aerobic methanotrophs have the potential to enhance carbonate dissolution and induce corrosion (Krause et al., 2014).

$$CH_4 + 2O_2 \rightarrow CO_2 + 2H_2O \quad (1)$$

Lipid biomarkers are a powerful tool to identify and classify aerobic methanotrophic bacteria in modern environments and in the rock record (e.g., Collister et al., 1993; Cordova-Gonzalez et al., 2020; Elvert & Niemann, 2008; Rush et al., 2016; Talbot et al., 2014). Biomarkers of aerobic methanotrophic bacteria are typically $^{13}C$-depleted to different degrees (Jahnke et al., 1999), providing additional evidence for an assignment to this group of source organisms. One example of seep carbonates with the coincidence of extensive corrosion features and abundant lipids of aerobic methanotrophic bacteria stems from northern Istria, Croatia (Natalicchio et al., 2015). The Istrian Eocene carbonates were found to contain characteristic $^{13}C$-depleted lanostanes ($\delta^{13}C$: −47‰), degradation products of 4-methyl and 4,4-dimethyl sterols of methanotrophic bacteria (Bouvier et al., 1976; Cordova-Gonzalez et al., 2020; Schouten et al., 2000). Another example with the same coincidence of rock fabric and biomarker inventory are the Cretaceous Tepee Buttes of the Western Interior Seaway (Birgel, Peckmann, et al., 2006), which were found to contain rearranged $^{13}C$-depleted hopanoids (e.g. $C_{34}$-8α(H),14a(H)-secohexahydrobenzohopane; $\delta^{13}C$: −110‰) probably resulting from biodegradation of bacteriohopanepolyols of aerobic methanotrophs (cf. Talbot et al., 2001). Besides hopanoids and 4-methyl and 4,4-dimethyl sterols, diagnostic biomarkers of aerobic methanotrophs include a suit of unsaturated and monounsaturated fatty acids with double bond positions at ω5, ω7, and ω8 (Hanson & Hanson, 1996). The common occurrence of characteristic lipids of aerobic methanotrophs in seep carbonates and sediments (Birgel et al., 2011; Birgel & Peckmann, 2008; Birgel, Thiel, et al., 2006; Elvert & Niemann, 2008; Himmler et al., 2015) confirms that aerobic methanotrophy is a prominent process in the seafloor and the water column in methane-seep environments. However, the effect of aerobic methanotrophy on carbonate dissolution in natural environments is currently only based on circumstantial evidence.

Here, we report on a corrosion and bioerosion experiment using limestone cubes deployed for 2.5 years at three locations within the REGAB seep field of the Gabon-Congo-Angola passive margin, including a mussel bed, a site with outcropping methane hydrate and active seepage, and a site with no apparent seepage for comparison. After sample recovery, the surfaces of cubes were inspected for carbonate corrosion and bioerosion, by identifying traces of microbioerosion on the limestone surfaces and in epoxy casts thereof using scanning electron microscopy. Adhering biofilms were scraped off the cubes and analyzed for their lipid biomarker inventories; additionally, samples showing signs of microbioerosion were analyzed by 16*S* *r*RNA gene sequencing targeting the bacterial population. The combination of obtained data allows us to make a case for carbonate corrosion caused by aerobic methanotrophic bacteria, supporting the hypothesis of aerobic methanotrophy as one of the triggers of carbonate corrosion at marine methane seeps.

## 2 | GEOLOGICAL SETTING

The giant REGAB Pockmark is an active seep field located at approximately 3160 m water depth on the Gabon-Congo-Angola passive margin, about 10 km to the north of the Congo deep-sea channel (Figure 1; Ondréas et al., 2005). The REGAB pockmark is above

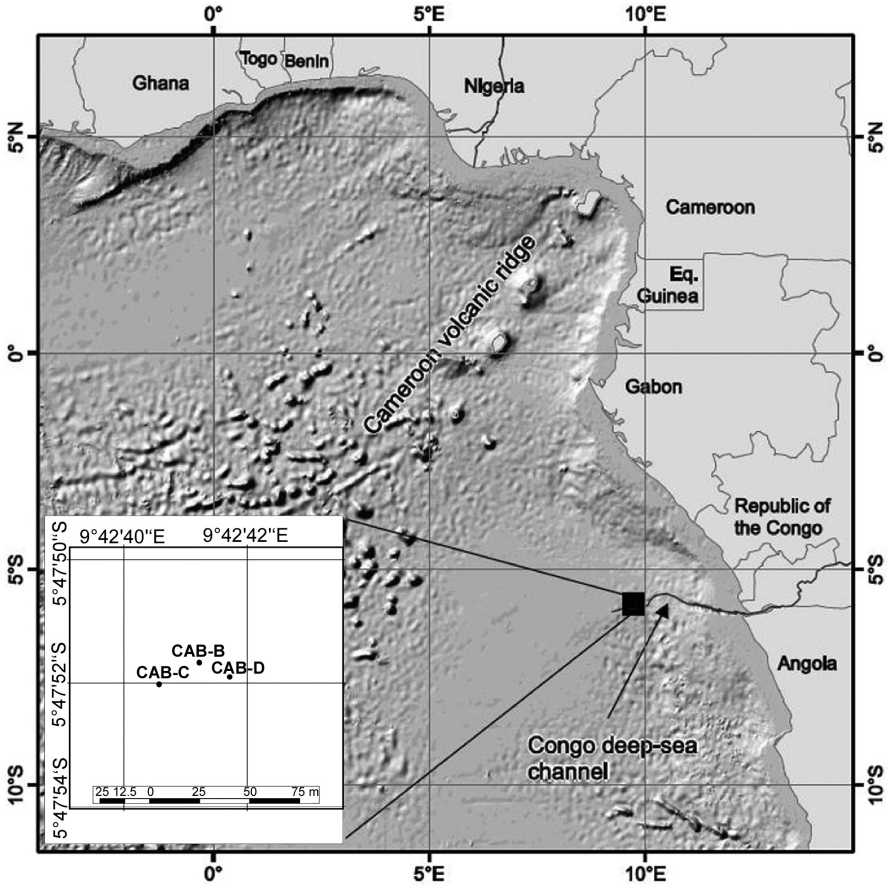


**FIGURE 1** Location of the study area within the REGAB Pockmark (after Marcon, Sahling, et al., 2014).

the carbon compensation depth (CCD), currently approximately at 5000 m in the Atlantic Ocean (Woosley, 2016), hence no physical–chemical dissolution occurs at the study site and carbonates can accumulate over long periods of time (Pop Ristova et al., 2012). The elliptical structure with diameters ranging between 700 and 950 m is composed of numerous depressions that are 0.5–15 m deeper than the surrounding seafloor (Marcon, Ondréas, et al., 2014). Remotely operated vehicle-borne micro-bathymetry and backscatter data of the entire structure, and high-resolution photo-mosaicking, side-scan sonar mapping of gas emissions, and maps of faunal distribution as well as of carbonate crust occurrence were combined to provide detailed information on fluid flow regimes in the subsurface (Marcon, Ondréas, et al., 2014). One prominent feature of the REGAB Pockmark is the presence of abundant authigenic carbonate (Ondréas et al., 2005; Pierre & Fouquet, 2007). Seismic profiles showed that the REGAB Pockmark is linked to a deep channel system that acts as a reservoir for seeping fluids by a 300-m deep chimney rooted in the channels, along which gas escapes (Ondréas et al., 2005). Gas seepage has been observed at several locations, and gas hydrates have been detected in the shallow subsurface at depths of 6 m or outcropping on the seafloor (Olu-Le Roy et al., 2007). The gas hydrates are composed mainly of biogenic methane (up to 99%) and traces of other gases, such as carbon dioxide, ethane, and hydrogen sulfide (Charlou et al., 2004), which sustain an abundant and diverse population of megafauna and microbial communities, including aerobic and anaerobic methanotrophs (Bouloubassi et al., 2009; Marcon, Sahling, et al., 2014). The methane gas was found to exhibit $\delta^{13}C$ values of −69.3‰ (Charlou et al. (2004).

## 3 | METHODS

Non-seep carbonate samples were deployed in three habitats within the REGAB seep field (Congo area) at ca. 3160 m water depth as part of the "corrosion and bioerosion" (CAB) experiment launched during cruise GUINECO M76/3b with the research vessel *Meteor* in July–August 2008 (Figure 2; Zabel et al., 2012). Experiment CAB-B was deployed in a mussel bed, experiment CAB-C was placed on an active seepage site with abundant chemosymbiotic benthos (mussels and tubeworms) and underlying gas hydrates; experiment CAB-D was deployed on the seafloor at a site where no evidence of seepage was recognized (Figure 2). Data on pore water geochemistry (hydrogen sulfide and methane fluxes) of the studied habitats at the REGAB pockmark were published by Olu-Le Roy et al. (2007) and Pop Ristova et al. (2012). The latter study used sediment samples and in situ geochemical measurements collected during the M76/3b cruise, when our CAB samples were deployed. These measurements included a mussel patch close to CAB-B, and bare sediments close to the carbonate deployment station CAB-D. Unfortunately, no sediment cores were taken and no biogeochemical measurements were made right at the carbonate site of CAB-C due to the hard substrate at this location and outcropping gas hydrates, accompanied

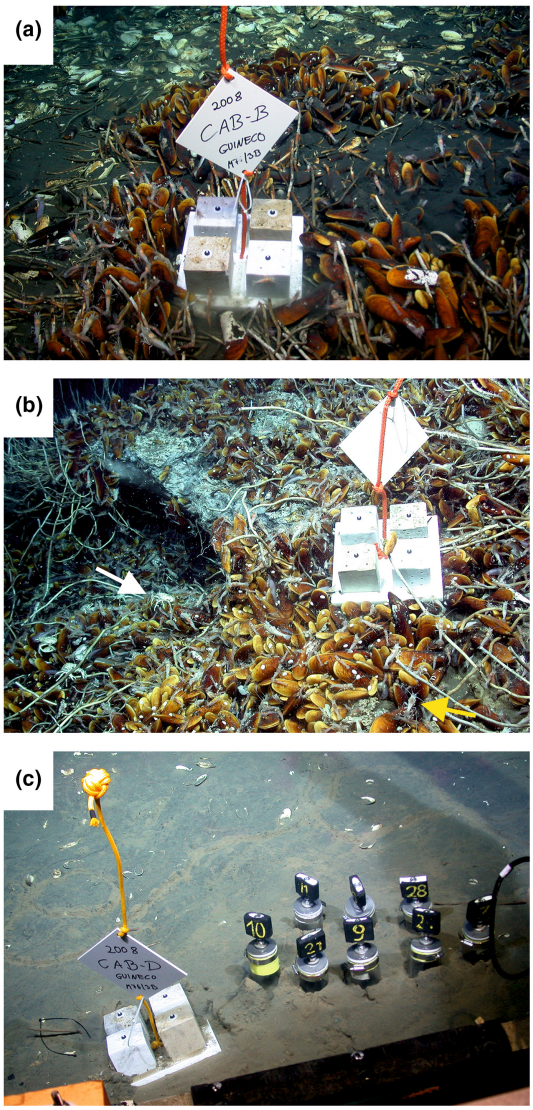


FIGURE 2 Carbonate experiments with four limestone cubes each, deployed for 2.5 years within the REGAB Pockmark in the Lower Congo Basin at ca. 3160 m water depth. (a) Upon deployment of CAB-B in a mussel bed, gas escaped from the sediment. (b) CAB-C placed onto an active hydrate site with mussels and tubeworms, yellow arrow indicating a shrimp, white arrow pointing to a crab. (c) CAB-D located in a reference area with no apparent seepage activity.

by vigorous methane gas efflux. Pore-water concentrations of hydrogen sulfide as well as hydrogen sulfide fluxes generally increased with increasing sediment depth at all study sites; with maximum concentrations detected at mussel beds close to CAB-B, where the hydrogen sulfide flux was 23 mmol $m^{-2}d^{-1}$ and the methane efflux 334 mmol $m^{-2}d^{-1}$, representing average values in 0–10 cm sediment depth. At the site close to CAB-D, the hydrogen sulfide flux was 7 mmol $m^{-2}d^{-1}$, methane efflux was not detectable (Pop Ristova et al., 2012). The hydrogen sulfide gas fluxes in the bottom water at REGAB were low or undetectable (Olu-Le Roy et al., 2007). Methane concentrations in the bottom waters (10 cm above seafloor), as well as methane fluxes and methane consumption rates, were highest in the vicinity of the mussel habitat (CAB-B), suggesting substantial transport of methane to the bottom water. The reference site (CAB-D) showed low contents of methane gas compared with CAB-B (Pop Ristova et al., 2012).

Each experiment was comprised of four limestone cubes with 10 cm side length, including two cubes of marble and two cubes of fossiliferous limestone, all of which were regularly pierced by vertical drill holes (Figure 2). Before deployment, the limestone cubes had been fixed on a square-cut plastic board (edge length 25 cm), which was regularly pierced by drill holes to allow for fluid flow through the equidistantly pierced limestone cubes. Each of the limestone cubes was attached to the plastic board by a central metal screw. The samples were retrieved in January–February 2011 during the West Africa Cold Seeps (WACS) cruise aboard the *R/V Pourquoi Pas?* (Olu, 2011). For this study, only the marble cubes have been used. The marble cubes were divided into subsamples for petrographic and organic geochemical analyses.

### 3.1 | Lipid biomarkers analyses

For lipid biomarker analyses, biofilms attached to the carbonate surfaces were scraped off with a razor blade. The surface coatings were gently grounded and hydrolyzed with 6% KOH in methanol to cleave ester-bond lipids, and then extracted with a mixture of dichloromethane/methanol (3:1, v/v) by ultrasonication until the solvents became colorless. An aliquot of the resulting lipid extracts was separated by column chromatography (using aminopropyl-bonded silica gel column) into four fractions: (1) hydrocarbons (*n*-hexane), (2) ketones (*n*-hexane/dichloromethane, 3:1, v/v), (3) alcohols (dichloromethane/acetone, 9:1, v/v), and (4) carboxylic acids (2% formic acid in dichloromethane; cf. Cordova-Gonzalez et al., 2020). Alcohols were analyzed as trimethylsilyl-ether derivatives and fatty acids as fatty acid methyl ester derivatives (cf. Birgel & Peckmann, 2008). The double bond position of monounsaturated fatty acids was determined by analysis of their dimethyl disulfide adducts following Nichols et al. (1986).

Lipid biomarkers were analyzed by means of gas chromatography–flame ionization detection (GC – FID) for quantification and gas chromatography–mass spectrometry (GC–MS) for identification using a Thermo Electron Trace MS instrument at the MARUM, University of Bremen, equipped with a R*xi*-5 MS fused silica capillary column (30 m, 0.25 mm inner diameter, 0.25 µm film thickness). The GC temperature program was: injection at 60°C (1 min) to 150°C at 10°C $min^{-1}$, then from 150°C to 320°C at 4°C $min^{-1}$, 37 min isothermal. The identification by GC–MS was based on GC retention times, comparison of mass spectra with published data, and coelution experiments. Internal standards (cholestane, 1-nonadecanol, 2-methyl-octadecanoic acid) with known concentrations were added prior to sample hydrolysis and extraction. Compound-specific carbon isotope analysis was performed using a Thermo Fisher Trace GC Ultra connected via a Thermo Fisher GC Isolink Interface to a Thermo Fisher Delta V Advantage isotope-ratio-monitoring mass

spectrometer (IRM – MS), at the Department of Terrestrial Ecosystem Research, University of Vienna, Austria. Compound-specific carbon isotope values are given as δ values in per mil (‰) relative to Vienna Peedee Belemnite (V-PDB). The $\delta^{13}C$ values of alcohols (TMS-derivatives) and carboxylic acids (methyl esters) were corrected for the additional carbons introduced during derivatization.

The conditions for GC – IRM – MS analyses were identical to those used for GC analyses. Each measurement was calibrated using several pulses of carbon dioxide gas with known composition at the beginning and the end of the run. The precision of measurements was checked with a mixture of *n*-alkanes ($C_{14}$-$C_{38}$) with known isotopic composition. The analytical standard deviation was smaller than 0.4‰.

### 3.2 | 16*S rRNA* gene sequencing

16*S rRNA* gene sequence analysis was performed on biofilms adhered to carbonates surfaces showing evidence of microbial corrosion (CAB-C). DNA was extracted from 0.2 g material using a phenol-chloroform extraction protocol previously described (Urich et al., 2008). 16*S rRNA* gene libraries of bacteria were constructed with primers 616 V and 1492R (Juretschko et al., 1998; Lane, 1991). The gel-purified PCR products were cloned into a pGEM-T Easy vector system (Promega, Mannheim, Germany) and positive clones were further processed and Sanger-sequenced at LGC Genomics (Berlin, Germany). Sequences were taxonomically classified with CREST (Lanzén et al., 2012). The sequences reported in this paper have been deposited in the GenBank database under accession numbers OM761078 - OM761163.

### 3.3 | Scanning electron microscopy

For studying traces of microbial microbioerosion, surfaces of the marble cubes were treated with hydrogen peroxide and cleaned in an ultrasonic bath to remove any organic biofilm. Surfaces were then examined with a Tescan VEGA3 xmu scanning electron microscope (SEM) at 15 keV using a secondary electron detector. Subsamples were embedded in epoxy resin under vacuum conditions in a Struers CitoVac impregnation chamber, followed by dissolution of the carbonate with hydrochloric acid (for further detail, see Wisshak, 2012), yielding epoxy casts with the positive infills of microbioerosion traces that were then analyzed with SEM after sputter-coating with gold.

## 4 | RESULTS

### 4.1 | Carbonate corrosion features

SEM surface examination of the marble cubes of experiment CAB-C showed the pristine coarsely crystalline texture of the carbonate rock and, in places, intense surface pitting indicative of microbioerosion (Figure 3a). Accordingly, the epoxy casts revealed clusters of microborings of a yet-unknown morphology (Figure 3b–f). These range from individual, circumradial tunnel systems (Figure 3b) to dense carpets of borings with little or no areas of pristine matrix between (Figure 3c, d). Close-up SEM micrographs showed that individual tunnels are ca. 2–3 µm in diameter and radiate from a central point of entry in all directions while repeatedly bi- or trifurcating in acute angles. These tunnels slightly expand toward their rounded terminations that may reach a diameter of up to 5 µm (Figure 3e, f). This new type of microboring with some affinity to the ichnospecies *Fascichnus bellafurcus* (Radtke et al., 2010), formerly *Abeliella bellafurca* (see Wisshak et al., 2019), is by far the dominant microboring in all the investigated samples, complemented only by very few, larger and strictly prostrate tunnels of the presumed fungal microboring *Orthogonum tubulare* (Radtke, 1991), a ubiquitous bioerosion trace in aphotic marine settings. Cubes CAB-B and CAB-D showed no signs of microbioerosion.

### 4.2 | Composition of the microbial community

16*S rRNA* gene sequencing was carried out to decipher the bacterial community in the biofilms attached to the corroded surface of the CAB-C marble cube from a hydrate-bearing active seep site (Figure 4), for which SEM analyses revealed evidence of microbioerosion. Biofilms were adhering to all cube surfaces exposed to seawater, including the upper surface. A total of 86 bacterial clones were detected (Table S1). Phylogenetic information shows that Proteobacteria predominate, accounting for 70% of the total clones. Among them, Gammaproteobacteria are the predominant class (62% of total clones; Figure 4a). The majority of the gammaproteobacterial community (Figure 4b) belongs to relatives of aerobic methanotrophs (i.e., Type I methanotrophs) of the order Methylococcales (38% of total clones; Figure 4c). Within this community, most methanotrophs are relatives of the uncultured clade Hyd24-01 (see Figure 4c), followed by relatives of the uncultured clade IheB2-23, and ecotypes of the family Methylococcaceae (now subdivided in Type Ia Methylomonadaceae and Type Ib Methylococcaceae; Parks et al., 2018), such as members of the genus *Methylomonas* (Table S1). Members of the class Gammaproteobacteria, known to be sulfide-oxidizing bacteria, were detected as well, accounting for 21% of the total clones. Detected sulfide-oxidizing bacteria include members of the order *Thiotrichales* (e.g., genera *Leucothrix* and *Thiothrix* of the family Thiotrichaceae) and *Chromatiales* (e.g., genus *Granulosicoccus* of the family Granulosicoccaceae).

### 4.3 | Lipid biomarkers

The lipid biomarker compound inventories of the hydrocarbon, alcohol, and fatty acid fractions of biofilms from the CAB-B, CAB-C, and CAB-D marble cubes are presented in Table 1.

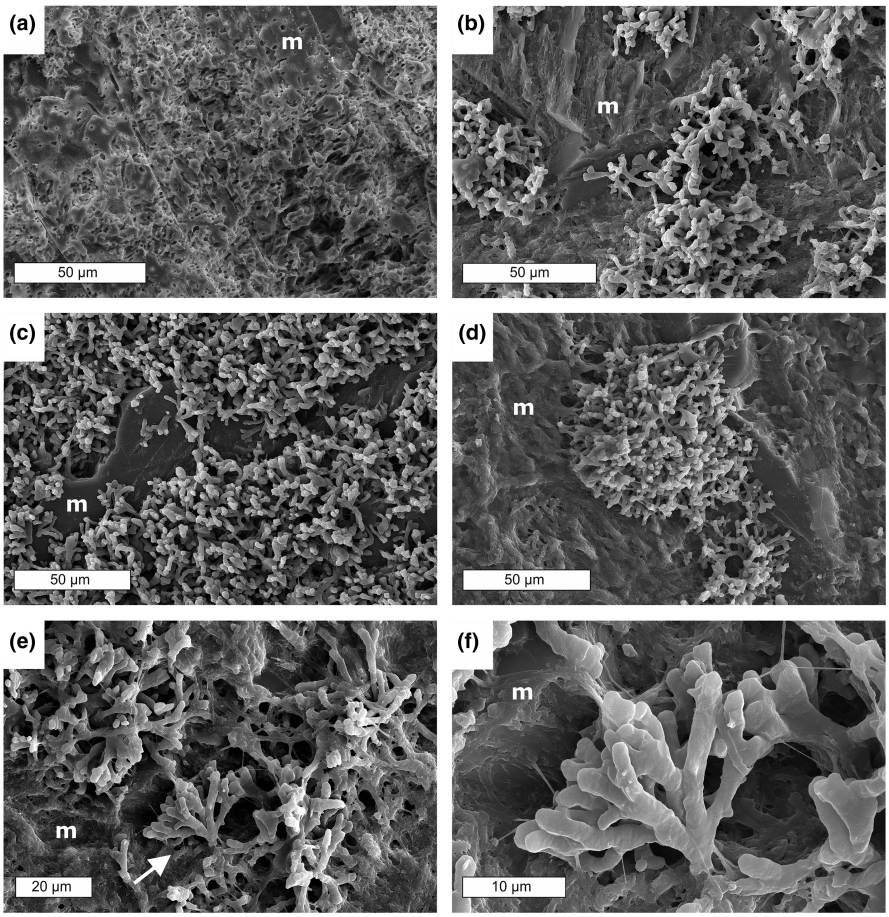


FIGURE 3 Scanning electron imaging of experimental marble substrates CAB-C (a) and epoxy casts thereof (b-f), showing distinctive signs of microbioerosion: (a) intense surface pitting in the coarsely crystalline carbonate matrix (m); (b) epoxy cast with circumradial microboring structure; (c-d) dense clusters of the same type of microboring; (e-f) close-ups of individual tunnels radiating and ramifying from a central point of entry toward slightly widened terminations.

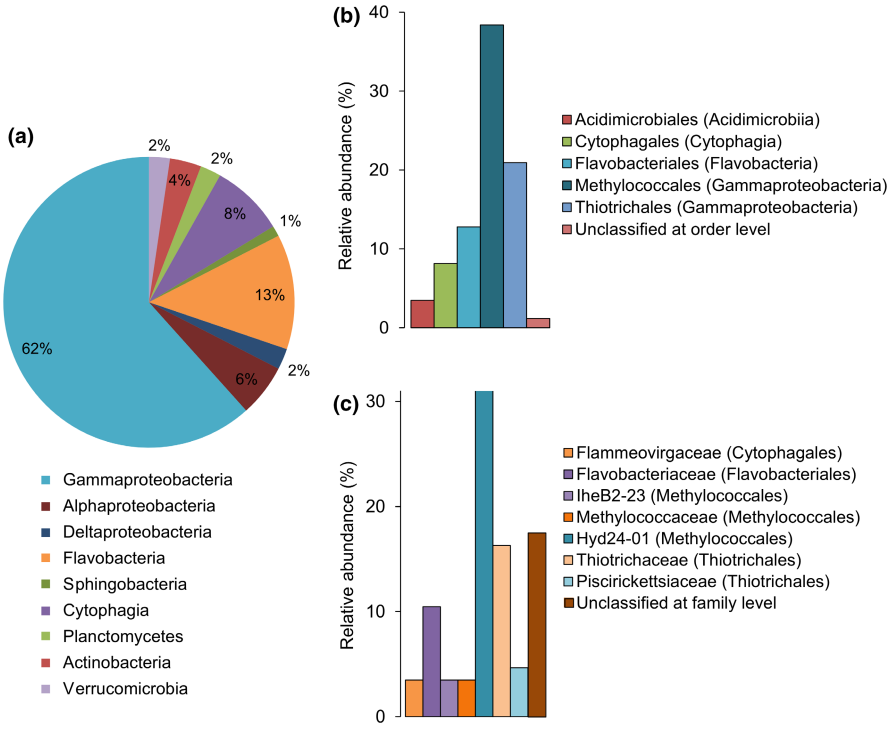


FIGURE 4 Diversity and relative abundance (%) of bacterial groups in the corroded surface of CAB-C. Each color represents the percentage of the total sample contributed by each taxon group at (a) phylum level, except for Proteobacteria and Bacteroidetes, which are shown by class; (b) order level (dominant phylotypes with relative abundance ≥3%), (c) family level (dominant phylotypes with relative abundance ≥3%).

Overall, highest contents of lipid biomarkers were detected for CAB-C (277.96 µg/g wet weight), followed by the reference sample CAB-D (61.84 µg/g), while lowest contents were found for CAB-B (48.48 µg/g). In all samples, fatty acids are the most abundant compounds, representing 87% of all lipid biomarkers in the CAB-B cube, 82% in CAB-C, and 96% in CAB-D. The second largest group

**TABLE 1** Contents (μg/g) and $\delta^{13}C$ (‰ vs V-PDB) values of lipid biomarkers from biofilms attached to CAB-B, CAB-C, and CAB-D cubes.

| | CAB-B | | CAB-C | | CAB-D | |
|---|---|---|---|---|---|---|
| | Content (μg/g ww) | $\delta^{13}C$ (‰ vs V-PDB) | Content (μg/g ww) | $\delta^{13}C$ (‰ vs V-PDB) | Content (μg/g ww) | $\delta^{13}C$ (‰ vs V-PDB) |
| *Alcohols* | | | | | | |
| Cholesterol **I** | 3.13 | −58 | 6.23 | −69 | 1.63 | −34 |
| Cholestanol **II** | | | 0.89 | n.m. | | |
| Desmosterol **III** | | | 12.59 | −77 | | |
| 4α-Methylcholest-8(14)-en-3β-ol **IV** | | | 0.62 | n.m. | | |
| 24-Methylcholesta-5,24(28)-dien-3β-ol **V** | 0.57 | n.m. | 4.14 | −76 | | |
| 4α-Methylcholesta-8(14),24-dien-3β-ol **VI** | | | 10.89 | −85 | | |
| Lanosterol **VII** | | | 1.77 | −76 | | |
| 4,4-Dimethylcholesta-8(14),24-dien-3β-ol **VIII** | | | 0.30 | n.m. | | |
| Cycloartenol **IX** | | | 2.51 | −68 | | |
| 4α-Methylcholest-8(14)-en-3β,25-diol **X** | | | 2.00 | −77 | | |
| Diplopterol **XI** | 1.91 | −76 | 3.20 | −84 | 0.34 | −61 |
| 17α(H),21β(H)-32-Hopanol **XIIa** | | | 1.65 | | | |
| 17β(H),21β (H)-32-Hopanol **XIIb** | | | 0.99 | | | |
| *Fatty acids* | | | | | | |
| $n\text{-}C_{14:0}$ | 4.17 | −51 | 10.58 | −56 | 6.17 | −29 |
| $n\text{-}C_{16:1\omega8c}$ | 8.00 | −76 | 68.51 | −69 | 4.59 | −71 |
| $n\text{-}C_{16:1\omega7c}$ | 3.94 | −69 | 39.38 | −60 | 3.47 | −60 |
| $n\text{-}C_{16:1\omega6c}$ | 1.30 | n.m. | 32.24 | n.m. | 2.65 | n.m. |
| $n\text{-}C_{16:1\omega7t\ \&\ 16:1\omega5c/t}$* | 2.78 | n.m. | 30.51 | n.m. | 2.17 | n.m |
| $n\text{-}C_{16:0}$ | 12.32 | −41 | 34.22 | −35 | 23.47 | −32 |
| $n\text{-}C_{18:1\omega9c}$ | 4.20 | −33 | 13.28 | −52 | 8.82 | −34 |
| $n\text{-}C_{18:1\omega7c}$ | 4.55 | −55 | 18.69 | −66 | 2.87 | coelution |
| $n\text{-}C_{18:0}$ | 3.88 | −35 | 9.95 | −59 | 7.65 | −30 |
| Total n-$C_{16}$ FA | 25.56 | | 174.35 | | 34.18 | |
| Total n-$C_{18}$ FA | 12.63 | | 41.91 | | 19.34 | |
| *Hydrocarbons* | | | | | | |
| 17α(H),21β(H)-25,28,30-Trisnorhopane | | | 0.57 | n.m. | | |
| 17β(H), 21β(H)-25-Norhopane | 0.13 | | 1.49 | −31 | | |
| Hop-17(21)-ene | 0.24 | | 0.37 | n.m. | 0.20 | |
| Diploptene | 0.14 | | 0.92 | −79 | | |
| Total lipid biomarkers | 48.48 | | 277.96 | | 61.84 | |

Abbreviations: n.m, not measured; ww, wet weight.

*Excluded from calculations due to coelution of $n\text{-}C_{16:1\omega7t}$, and $n\text{-}C_{16:1\omega5c/t}$ with $n\text{-}C_{16:2}$ on GC-FID.

are alcohols, representing 12% in CAB-B, 17% in CAB-C, and 3% in CAB-D. Hydrocarbons were detected in trace amounts in all samples, making up less than 3% of the total lipid biomarkers. Hopanoids and steroids dominate the alcohol and hydrocarbon fractions. Among fatty acids (including combined free and phospholipid derived fatty acids), saturated and monounsaturated

compounds with 16 and 18 carbon atoms are of particular interest (Figure 5). These compounds are the dominant fatty acids of aerobic methanotrophs (Hanson & Hanson, 1996), and the most abundant fatty acids in the samples (>75% of fatty acid content). For the calculation of the fatty acid percentages, only saturated and monounsaturated fatty acids with 14, 16, and 18 atoms were considered (Table 1).

### 4.3.1 | CAB-B (mussel bed)

In the hydrocarbon fraction of sample CAB-B, the most abundant lipid is hop-17(21)-ene (47%). 17β(H),21β(H)-30-norhopane and diploptene are also present in this fraction, representing approximately 25% each. The alcohol fraction is dominated by sterols, comprising cholesterol (56%) and 24-methylcholesta-5,24(28)-dien-3β-ol (10%). The only hopanoid detected in the alcohol fraction is diplopterol (34%; Figure 6). The fatty acid fraction of CAB-B is dominated by monounsaturated fatty acids (52% of the fraction). The distribution of saturated fatty acids in order of decreasing abundance is $n$-$C_{16:0}$ (29%), $n$-$C_{14:0}$ (10%), and $n$-$C_{18:0}$ (9%). The most prominent monounsaturated fatty acids are $n$-$C_{16:1\omega8c}$ (19%), followed by $n$-$C_{18:1\omega7c}$ (11%), $n$-$C_{18:1\omega9c}$ (10%), $n$-$C_{16:1\omega7c}$ (9%), and $n$-$C_{16:1\omega6c}$ (3%; Figure 6).

The $\delta^{13}C$ values of selected fatty acids (Table 1, Figure 6) vary from −76‰ ($n$-$C_{16:1\omega8}$) to −33‰ ($n$-$C_{18:1\omega9}$). Monounsaturated fatty acids $n$-$C_{16}$ have the lowest $\delta^{13}C$ values (average −72‰). In the alcohol fraction, $\delta^{13}C$ values range between −76‰ (diplopterol) and −58‰ (cholesterol). The $\delta^{13}C$ values of hydrocarbons were not measured due to too low contents.

### 4.3.2 | CAB-C (active seepage site with abundant mussels and tubeworms)

The most abundant hydrocarbon in the sample CAB-C is 17β(H), 21β(H)-30-norhopane (44%, Figure 6). Diploptene (27%),

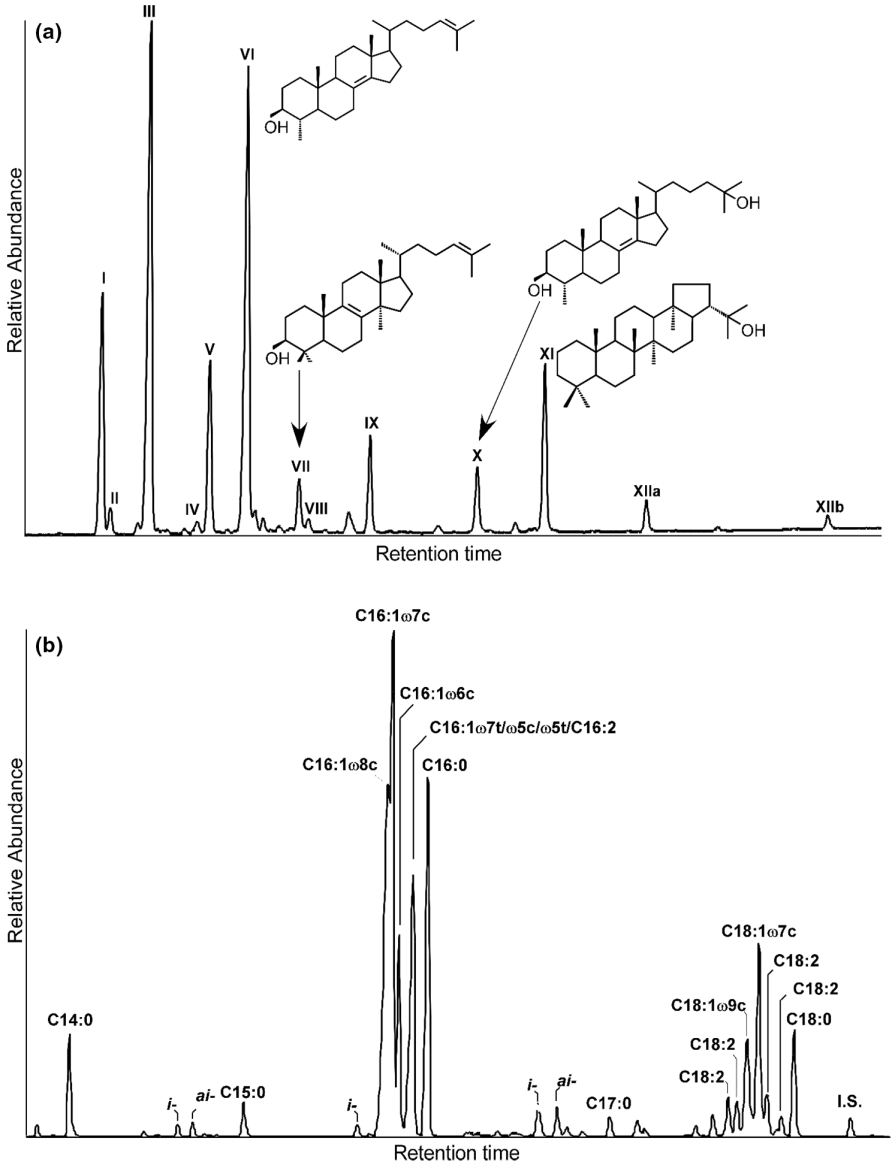


FIGURE 5 Partial gas chromatograms of alcohol (a) and fatty acid (b) fractions of CAB-C biofilm. *i* = *iso*, *ai* = *anteiso*. Roman numbers in (a) explained in Table 1.

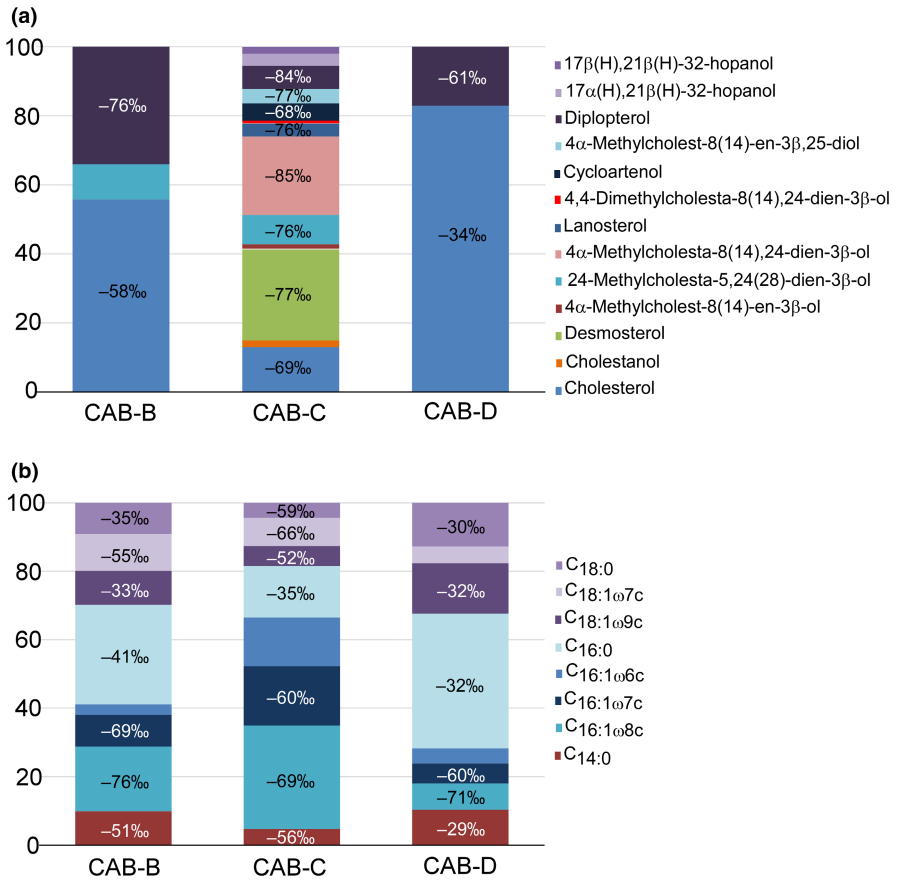


**FIGURE 6** Relative abundance of lipids in the alcohol (a) and fatty acid (b) fractions of biofilms from CAB-B, CAB-C, and CAB-D marble cubes. Values within each stacked column represent $\delta^{13}C$ values of lipids. $\delta^{13}C$ value of *n*-$C_{16:1\omega6c}$ not provided due to coelution with $C_{16:1\omega7c}$ on GC – IRM – MS.

17α(H),21β(H)-25,28,30-trisnorhopane (17%), and minor amounts of hop-17(21)-ene (11%) were detected as well (Table 1). In the alcohol fraction, sterols account for 88% of all compounds. Most abundant sterols are desmosterol (26%), various 4-methyl and 4,4-dimethyl sterols (25%), cholesterol (13%), and 24-methylcholesta-5,24(28)-dien-3β-ol (9%; Figure 6). Besides the commonly reported 4-methyl and 4,4-dimethyl sterols (4α-methylcholest-8(14)-en-3β-ol, 4α-methylcholesta-8(14),24-dien-3β-ol, 4,4-dimethylcholesta-8(14),24-dien-3β-ol), minor amounts of the unusual 4α-methylcholest-8(14)-en-3β,25-diol (4%) were detected, a compound that was first described by Elvert and Niemann (2008) from Haakon Mosby Mud Volcano sediments. Further sterols include cycloartenol, lanosterol, and cholestanol (Table 1, Figure 5). Few hopanoids were detected in the alcohol fraction, including diplopterol (7%), and 17α(H),21β(H)- and 17β(H),21β (H) isomers of $C_{32}$-hopanol (bishomohopanol; 5%). The fatty acid fraction of CAB-C is dominated by monounsaturated fatty acids, representing 76% of the selected saturated and unsaturated fatty acids comprising 14, 16, and 18 carbons (see chapter 4.3). In sample CAB-C, the most abundant fatty acid is *n*-$C_{16:1\omega8c}$ (30%) followed by *n*-$C_{16:1\omega7c}$ (17%) and *n*-$C_{16:1\omega6c}$ (14%; Figure 6). Monounsaturated fatty acids with 18 carbon atoms, *n*-$C_{18:1\omega7c}$ (8%), and *n*-$C_{18:1\omega9c}$ (6%) are present in smaller amounts. Fatty acids *n*-$C_{16:0}$ (15%), *n*-$C_{14:0}$ (5%), and *n*-$C_{18:0}$ (4%) are present as well, although they are less prominent than the respective monounsaturated compounds (Table 1, Figure 5).

Diploptene shows the lowest $\delta^{13}C$ value (−79‰) among the hydrocarbons, while the other measured compound, 17β(H),21β(H)-30-norhopane, is considerably less $^{13}C$-depleted with a $\delta^{13}C$ value of −31‰. In the alcohol fraction, diplopterol exhibits the lowest $\delta\ ^{13}C$ value (−84‰). Among sterols, the lowest $\delta\ ^{13}C$ value was found for 4α-methylcholesta-8(14),24-dien-3β-ol (−85‰), whereas cholesterol and cycloartenol show the highest values (average − 68‰). The $\delta^{13}C$ values for other sterols vary between −77‰ and − 76‰ (Table 1, Figure 6). Fatty acids were found to be considerably less depleted than alcohols (Table 1, Figure 6). The most $^{13}C$-depleted fatty acids are monounsaturated fatty acids *n*-$C_{16}$ (average − 65‰) and *n*-$C_{18:1\omega7}$ (−66‰). The highest $\delta^{13}C$ value was found for *n*-$C_{16:0}$ (−33‰).

### 4.3.3 | CAB-D (reference site)

The only hydrocarbon detected in the reference sample CAB-D is hop-17(21)-ene. In the alcohol fraction, only cholesterol and diplopterol are present (83% and 17% of the fraction, respectively). The fatty acids are dominated by saturated fatty acids (62%). *n*-$C_{16:0}$ (39%) is the most abundant fatty acid, followed by *n*-$C_{18:0}$ (13%) and *n*-$C_{14:0}$ (10%). Monounsaturated fatty acids represent 38% of the fraction, including *n*-$C_{16:1\omega8c}$ (8%), *n*-$C_{16:1\omega7c}$ (6%), *n*-$C_{16:1\omega6c}$ (4%), *n*-$C_{18:1\omega9c}$ (15%), and *n*-$C_{18:1\omega7c}$ (5%; Table 1, Figure 6).

The $\delta^{13}C$ values of alcohols in reference sample CAB-D (Table 1, Figure 6) fall between −61‰ (diplopterol) and −34‰ (cholesterol). The $\delta^{13}C$ values of fatty acids vary widely from −71‰ to −30‰.

No $\delta^{13}C$ values were obtained for compounds of the hydrocarbon fraction due to too low contents.

## 5 | DISCUSSION

Some biogeochemical processes strongly affect the carbonate system in sedimentary environments by the production or consumption of protons and the production of carbonate species (Coleman, 1993), causing either the formation of authigenic carbonate minerals or the dissolution of skeletal or authigenic carbonate in the sediment or at the sediment surface. Apart from such effects driven by the metabolism itself, extracellular polymeric substances (EPS) are known to affect the carbonate system (Dupraz et al., 2009). Microbial sulfate reduction is an example to highlight that the effect of a biogeochemical process is not straightforward. It depends on factors including (1) environmental conditions (e.g., presence and speciation of iron), (2) the types of electron donors metabolized, and (3) EPS composition if sulfate reduction results in carbonate formation or dissolution (Baumann et al., 2016; Gallagher et al., 2014; Meister, 2013). The effects of other biogeochemical processes on the carbonate system are more straightforward. This includes the calcium pump (i.e., ATPase-mediated transcellular $Ca^{2+}$ transport) of cyanobacteria (Garcia-Pichel, 2006; Garcia-Pichel et al., 2010), which is one of the mechanisms, apart from local acidification caused by respiration, that might also apply for other agents of microbial bioerosion in marine environments. With respect to marine methane seeps, aerobic methanotrophy and sulfide oxidation have been held responsible for carbonate dissolution (Himmler et al., 2011; Matsumoto, 1990). Yet, experiments to assess the effect of biogeochemical processes on the carbonate system in marine methane-rich environments are scarce.

### 5.1 | Were aerobic methanotrophic bacteria corroding carbonate at the REGAB seep field?

The SEM analyses revealed evidence of microbioerosion associated with the presence of biofilms adhering to the carbonate substrate of cube CAB-C, which was exposed to active methane seepage and outcropping hydrates for 2.5 years. As expected, reference site CAB-D revealed no evidence of active seepage and respectively no signs of bioerosion. For CAB-B, where methane and hydrogen sulfide flux was measured when the samples were deployed (see Olu-Le Roy et al., 2007; Pop Ristova et al., 2012), no bioerosion was recognized. Possibly, the lack of bioerosion for the latter site was caused by temporal variability or even episodical cessation of seepage, indicated by a lower density of the local mussel population with smaller size of mussels compared with other mussel-dominated sites at the REGAB Pockmark (cf. Olu-Le Roy et al., 2007). In fact, CAB-B might represent an older mussel assemblage related to lower methane flux (cf. Olu-Le Roy et al., 2007), which could be one of the reasons why only the marble cube at the high flux, mussel-inhabited CAB-C site was affected by microbioerosion. Such pattern provides circumstantial evidence for a methane-dependent bioerosion process in case of the CAB-C cube, given the dominance of aerobic methanotrophs in the adhering biofilm suggested by 16*S* *r*RNA genes and lipid biomarker data. This line of reasoning receives further support from the observation of a nearly monoichnospecific bioerosion trace assemblage with the dominant microbioerosion trace being new to science and having a very high abundance in the samples studied. These microbioerosion traces have been formed in a purely inorganic substrate (marble), being of limited attraction for organotrophic microendoliths such as marine fungi, which would have been expected in a much higher abundance and diversity in a biogenic substrate (e.g., skeletal carbonate) after more than 2 years of exposure in this aphotic environment (cf. Golubic et al., 2005; Wisshak et al., 2011). Together, the ichnological observations suggest that the dominant agent of microbioerosion observed in the marble cubes exposed to active seepage is a bacterium with a methane- or hydrogen sulfide-based metabolism.

Even at the most active seeps, hydrogen sulfide tends to be completely oxidized at the seafloor, and its concentration in the bottom water is typically much lower than the concentration of methane (Boetius & Wenzhöfer, 2013; Niemann et al., 2005; Sahling et al., 2002), as for the REGAB seep, where concentrations of hydrogen sulfide in the bottom water (Olu-Le Roy et al., 2007) and sediment surface layers were low (Pop Ristova et al., 2012), while high methane concentrations were found in the mussel dominated sites (Pop Ristova et al., 2012). Consequently, the position of the marble surfaces some centimeters above the seafloor, together with the moderate fluid flow restriction caused by the perforated plastic boards and marble cubes, seems to have favored aerobic methanotrophy rather than sulfide oxidation.

Aerobic methanotrophy commonly occurs at methane seeps (Birgel et al., 2011; Birgel & Peckmann, 2008; Birgel, Thiel, et al., 2006; Cordova-Gonzalez et al., 2020; Elvert & Niemann, 2008; Himmler et al., 2015; Kellermann et al., 2012). The composition of a community of aerobic methanotrophs can be assessed by phylogenetic analyses and lipid biomarkers (Hanson & Hanson, 1996). In this respect, the bioeroded surface of the marble cubes in the CAB-C experiment and the close to exclusive occurrence of a new type of microbioerosion trace suggest that site-specific microorganisms were involved in carbonate corrosion. Based on 16*S* *r*RNA gene analysis, aerobic methanotrophs of the order Methylococcales were among the most abundant bacteria identified. Among the Methylococcales, relatives of the Hyd24-01 clade, followed by the IheB2-23 clade, and representatives of the genus *Methylomonas* were most abundant. To date, no pure cultures of bacteria of the Hyd24-01 clade exist; however, this clade has been reported from other methane-rich sites, including surface sediments of Haakon Mosby Mud Volcano (Lösekann et al., 2007). The uncultured clade IheB2-23 was first detected in the water column of the northern South China Sea (Mau et al., 2020).

Apart from aerobic methanotrophs, the CAB-C biofilms contained abundant Thiotrichales. These and other sulfide-oxidizing bacteria are potential candidates other than aerobic methanotrophs

that may have caused the observed microbioerosion of marble. The biomarker inventory of the CAB-C biofilms helps to further evaluate the phylogenetic affiliation of the microbioeroder. Although, lipid biomarkers are affected by taphonomic processes (e.g., Xie et al., 2013), the circumstance that active biofilms have been sampled renders it unlikely that the obtained lipid inventory was compromised by degradation processes. Biomarkers are therefore suitable to determine the microorganisms that dominated the CAB-C biofilms and to identify the probable bioeroder.

The lipid biomarker inventory of the biofilm adhering to the CAB-C marble chiefly includes fatty acids, accompanied by 4-methyl and 4,4-dimethyl sterols and hopanoids, most of them commonly reported from aerobic methanotrophic bacteria. The fatty acid profile of the CAB-C biofilm is dominated by *n*-$C_{16:1\omega8}$ ($\delta^{13}C$: −69‰). This lipid biomarker is known to be produced only by Type I methanotrophic bacteria (Bowman, 2006; Willers et al., 2015), including members of the genus *Methylomonas* (Hanson & Hanson, 1996), detected by 16*S* *r*RNA gene sequencing. Another fatty acid related to Type I methanotrophs of the genus *Methylomonas* is *n*-$C_{16:1\omega5t}$, which represents an excellent environmental marker for aerobic methanotrophy (Bowman, 2006; Willers et al., 2015).

Abundant *n*-$C_{16:1\omega7}$ ($\delta^{13}C$: −60‰), a fatty acid found in high concentration in *Methylomonas* strains (Bowman, 2006), is a ubiquitous fatty acid sourced by many organisms including algae and bacteria such as sulfide-oxidizing bacteria (McCaffrey et al., 1989). Thiotrichales, sulfide-oxidizing bacteria, were among the Gammaproteobacteria in the 16*S* *r*RNA gene analyses of the CAB-C biofilm. However, based on the presence of ω8 unsaturated fatty acids and the $\delta^{13}C$ values of *n*-$C_{16:1\omega7}$, aerobic methanotrophs are the most likely source organisms of this compound since lipids of sulfide-oxidizing bacteria are typically less $^{13}C$-depleted than lipids of aerobic methanotrophs (Kellermann et al., 2012; Pond et al., 1998).

The observed high contents of *n*-$C_{18:1\omega7c}$ fatty acid ($\delta^{13}C$: −66‰) are surprising since this compound is considered a biomarker of Type II methanotrophs (Alphaproteobacteria), and the 16*S* *r*RNA gene analysis yielded only sequences of gammaproteobacterial methanotrophs. Similar inconsistencies were found by Kellermann et al. (2012) when studying mussel symbionts from *B. childressi* collected at a hydrocarbon seep in the Gulf of Mexico. The authors found a lipid composition consistent with Type II methanotrophs; yet, only sequences of Type I methanotrophs were detected with the 16*S* *r*RNA gene analysis. Although Type I methanotrophs are the dominant methanotrophs in marine environments, there are reports of Type II methanotrophs from the Black Sea water column, accounting for up to 10% of the methanotrophic population (Durisch-Kaiser et al., 2005). Moreover, despite the common use of fatty acid profiles to distinguish between Type I and II methanotrophs, most members of the family Methylothermaceae (Type I: *Methylohalobius crimeensis*, *Methylothermus subterraneaus*, and *Methylomarinovum caldicuralii*), some of them isolated from marine environments, produce significant amounts of *n*-$C_{18:1\omega7c}$ (Knief, 2015). Since similar fatty acid profiles have been described for Type I and II methanotrophs (e.g., Knief, 2015), additional evidence is needed for such comparison. The assignment of *n*-$C_{18:1\omega7c}$ fatty acid to a source organism is further complicated by the circumstance that this compound is also produced by sulfide-oxidizing bacteria (McCaffrey et al., 1989), and possibly by other bacteria identified in the biofilm attached to the carbonate, since this fatty acid is produced by many organisms. Its low $\delta^{13}C$ value rather agrees with aerobic methanotrophs as dominant source microorganisms (cf. Kellermann et al., 2012; Pond et al., 1998), although mixed input from both groups cannot be excluded.

Additional evidence for the assignment of the biota of the CAB-C biofilms comes from sterols and hopanoids (Ourisson et al., 1979, 1987). Sterols are valuable biomarkers in marine systems and sediments, reflecting input from multiple sources. Some sterols, such as cholesterol, cholestanol, desmosterol, and 24-methylcholesta-5,24(28)-dien-3β-ol, have been previously reported to occur in seep carbonates; yet, the sources of these compounds are mostly unspecific (Guan et al., 2021). On the other hand, 4-methyl and 4,4-dimethyl sterols (4α-methylcholest-8(14)-en-3β-ol, 4α-methylcholesta-8(14),24-dien-3β-ol, 4,4-dimethylcholesta-8(14),24-dien-3β-ol) are of high specificity for aerobic methanotrophic bacteria. These compounds are produced by few bacteria only, including several strains of methanotrophs (*Methylosphaera hansonii*: Schouten et al., 2000; *Methylobacter luteus*, *Methylobacter whittenburyi*, *Methylococcus capsulatus*, *Methylosarcina lacus*: Wei et al., 2016; *Methylotuvimicrobium kenyense*, *Methylotuvimicrobium alcaliphilum*: Cordova-Gonzalez et al., 2020). $^{13}C$-depleted 4-methyl and 4,4-dimethyl sterols produced by aerobic methanotrophs have been detected in seep carbonates from the Gulf of Mexico (Birgel et al., 2011), sediments from Haakon Mosby Mud Volcano (Elvert & Niemann, 2008), and mussel gills (*Bathymodiolus childressi*, *Bathymodiolus brooksi*) hosting methane-oxidizing symbionts (Kellermann et al., 2012). The low $\delta^{13}C$ values of 4-methyl sterols (4α-methylcholesta-8(14),24-dien-3β-ol: −85‰ and 4α-methylcholest-8(14)-en-3β,25-diol: −77‰) of the CAB-C biofilms agree with methanotrophic bacteria as source organisms.

Of special interest is the presence of the uncommon sterol 4α-methylcholest-8(14)-en-3β,25-diol ($\delta^{13}C$: −77‰) in the CAB-C biofilm, a compound first reported from surface sediments from Haakon Mosby Mud Volcano (Elvert & Niemann, 2008) and assigned to aerobic methanotrophs. Remarkably, 16*S* *r*RNA gene analyses of Haakon Mosby sediments revealed the dominance of Methylococcales strains divided into two clusters, one of which closely related to the Hyd24-01 clade (Lösekann et al., 2007), the dominant clade in the CAB-C biofilm. This study is only the second report of 4α-methylcholest-8(14)-en-3β,25-diol. Our new finding suggests that this uncommon sterol is a lipid biomarker of the Hyd24-01 clade. Lanosterol, also present in the sample CAB-C surface, is thought to be a precursor of 4-methyl and 4,4-dimethyl sterols (Bouvier et al., 1976; Summons et al., 2006); to date, only its diagenetic product lanostane has been identified in ancient seep carbonates (Birgel & Peckmann, 2008; Natalicchio et al., 2015; Sandy et al., 2012). Hopanoids commonly occur in aerobic methanotrophic bacteria, especially bacteriohopanepolyols (Talbot et al., 2001). In the CAB-C

biofilm, the only abundant hopanoid was diplopterol, which is similarly $^{13}$C-depleted as the associated 4-methyl and 4,4-dimethyl sterols and therefore is also assigned to methanotrophic bacteria.

Biomarkers of aerobic methanotrophs are typically $^{13}$C-depleted due to fractionation relative to the already $^{13}$C-depleted methane source. Thus, compound-specific isotope composition represents a valuable tool for the interpretation of biomarkers of methanotrophs in recent and ancient environments (Cordova-Gonzalez et al., 2020; Jahnke et al., 1999). Considering a $\delta^{13}C_{methane}$ value of ca. −69‰, measured in shallow gas hydrates recovered from the REGAB Pockmark (Charlou et al., 2004), the fractionation ($\Delta\delta^{13}C$) between methane and biomarkers of aerobic methanotrophs averages −12‰ (from −16‰ to −7‰) for steroids and hopanoids. Previous studies on cultures of aerobic methanotrophs revealed a fractionation of terpenoids relative to methane ($\Delta\delta^{13}C_{terpenoids\text{-}methane}$) of −16‰ and − 25‰ for Type I *M. alcaliphilum* and *M. kenyense*, respectively (Cordova-Gonzalez et al., 2020), and − 1‰ for Type II *M. trichosporium* (Jahnke et al., 1999), in accordance with the $\Delta\delta^{13}C_{terpenoids\text{-}methane}$ found for the CAB-C biofilms herein. Yet, the $\Delta\delta^{13}C$ of fatty acids relative to methane is +6‰ on average (from 0‰ to +13‰). Such $^{13}$C enrichment is best explained by cellular physiology and intermediate metabolites causing fatty acids to be $^{13}$C-enriched relative to hopanoids in methanotrophs (cf. Jahnke et al., 1999) or by additional input of ω7 fatty acids from sulfide-oxidizing bacteria.

Both aerobic methanotrophy and sulfide oxidation potentially lower the pH and have the potential to induce carbonate corrosion (Leprich et al., 2021; Matsumoto, 1990). However, considering the presence and abundance of $^{13}$C-depleted fatty acids (*n*-$C_{16:1\omega8c}$, *n*-$C_{18:1\omega8c}$, *n*-$C_{16:1\omega5t}$), 4-methyl and 4,4-dimethyl sterols, and diplopterol, aerobic methanotrophic bacteria dominate the CAB-C biofilm. Together with the predominance of aerobic methanotrophs revealed by 16*S rRNA* gene analyses and the supposedly greater potential for methane oxidation rather than sulfide oxidation several centimeters above the seafloor on the surface of the exposed marble cubes (cf. Boetius & Wenzhöfer, 2013; Niemann et al., 2005; Sahling et al., 2002), the observed bioerosion below the CAB-C biofilm was probably caused by methanotrophic bacteria, whereas sulfide-oxidizing bacteria are apparently subordinate members of the CAB-C biofilm community.

### 5.2 | Carbonate microbioerosion and aerobic methanotrophy

Our carbonate corrosion experiment in the REGAB seep field confirms that carbonate rocks are susceptible to corrosion when exposed to methane seepage in an oxic environment. The corrosion surfaces, in this case microbioerosion traces, were found to be associated with biofilms dominated by aerobic methanotrophic bacteria. After 2.5 years of exposure to a seepage environment, the CAB-C marble blocks were found to exhibit densely pitted surfaces resulting from microbioerosion. The CAB-C trace fossil (Figure 3) has not previously been reported elsewhere. Pitting was apparently a chemically driven process, supposedly relying on a metabolism that produced acidity. It cannot be excluded that the trace maker used organic acids or chelating compounds in addition to metabolites or, possibly, took advantage of the chemical environment created in the biofilm (low pH caused by aerobic methanotrophy and subordinate sulfide oxidation), but was not a methanotroph or thiotroph itself. Based on our data, the phylogenetic affiliation cannot be assessed with certainty and a better understanding of this new type of microbioerosion requires further studies. However, the new data of the CAB experiment, specifically the bioerosion observed in CAB-C, support the hypothesis that aerobic methanotrophy at seeps can be closely associated with substantial carbonate corrosion.

Abundant corrosion surfaces had already been identified in ancient seep carbonates also found to contain biomarkers of aerobic methanotrophs (Birgel, Peckmann, et al., 2006; Natalicchio et al., 2015). In some instances, lacking biomarker evidence, corrosion of seep carbonates was attributed to aerobic methanotrophy (Aloisi et al., 2000), sulfide oxidation (Campbell et al., 2002), or a combination thereof (Himmler et al., 2011). Examples of carbonate corrosion in modern seep environments stem from the Mediterranean Sea, such as the Amsterdam and Athina Mud Volcanoes (Himmler et al., 2011) and the Nadir Brine Lake (Aloisi et al., 2000). Laboratory experiments conducted by Krause et al. (2014) demonstrated the potential of aerobic methanotrophy to affect carbonate stability, facilitating dissolution. The addition of cells of the methanotrophic bacterium *Methylosinus trichosporium* under saline conditions led to considerable calcite dissolution caused by the production of carbon dioxide (Equation 1). Cai et al. (2006) deployed bivalve shells in an experiment over 8 years at two locations in the Gulf of Mexico—an active hydrocarbon seep and a site unaffected by seepage. Shells exposed to seepage were substantially affected by carbonate corrosion. Carbon mass balances led the authors to conclude that aerobic oxidation of methane was the dominant mechanism lowering the porewater pH and consequently causing carbonate dissolution. Our experiment in the REGAB seep field supports this interpretation, providing new microtextural, phylogenetic, and biomarker evidence for the role of aerobic methanotrophy in carbonate corrosion at methane seeps.

Given the current concern about climate change and resultant ocean acidification, it becomes pertinent to pay more attention to the mechanisms involved in carbonate dissolution including microbially driven corrosion. More research, and in particular more laboratory studies (e.g., Leprich et al., 2021), should be conducted to understand the mechanisms and the dynamics of carbonate corrosion and microbioerosion. With seawater on a projected trend of declining pH, the demand on quantitative estimates of the influence of aerobic methanotrophy and other biogeochemical processes on carbonate corrosion – a process sequestering carbon dioxide as seawater bicarbonate – in marine environments is increasing.

## 6 | CONCLUSIONS

A carbonate corrosion experiment conducted over the course of 2.5 years in the REGAB seep field confirms that carbonate rocks

exposed to methane seepage are susceptible to corrosion when exposed to oxic conditions. After retrieval, purely inorganic marble cubes were found to be covered by biofilms dominated by aerobic methanotrophic bacteria. Underneath biofilms, marble surfaces of the CAB-C experiment, exposed to active methane seepage, were affected by corrosion, more precisely microbioerosion. The discovered microbioerosion trace with its circumradial tunnels, ca. 2–3 μm in diameter and radiating from a central point of entry while repeatedly bi- or trifurcating in acute angles, is new to science. The genetic data obtained from biofilms reflect the dominance of Type I aerobic methanotrophs of the order Methylococcales; among these, most methanotrophs are relatives of the uncultured clade Hyd24-01. Similar to the genetic data, the biofilm's lipid biomarker inventory including abundant $^{13}$C-depleted fatty acids (*n*-$C_{16:1\omega8c}$, *n*-$C_{18:1\omega8c}$, *n*-$C_{16:1\omega5t}$), 4-methyl and 4,4-dimethyl sterols, and diplopterol suggests a close tie between methanotrophs and their acidity-generating metabolism and microbioerosion; however, our data do not allow for the assignment of the trace maker to a certain phylogenetic affiliation. This study is only the second report of the uncommon sterol 4α-methylcholest-8(14)-en-3β,25-diol. As for the first report of this compound, it is associated with abundant methanotrophs of the Hyd24-01 clade. Such coincidence renders it likely that 4α-methylcholest-8(14)-en-3β,25-diol is a biomarker for the Hyd24-01 clade. The microtextural, phylogenetic, and biomarker evidence compiled during the examination of the REGAB carbonate corrosion experiment supports the concept of aerobic methanotrophy as a potent trigger of carbonate corrosion at marine methane seeps.

## ACKNOWLEDGMENTS

We thank the German Academic Exchange Service – DAAD, which supported Alexmar Cordova-Gonzalez with a doctoral fellowship, Lars Hoffmann-Sell (MARUM Bremen) for assistance in sample preparation and analyses, and our colleagues Antje Boetius, chief scientist during RV *Meteor* cruise M56/3b, and Karine Olu, chief scientist during the WACs cruise on RV *Pourquoi pas?*, for allocation of diving time to deploy and recover the experiments at the seafloor. Insightful comments provided by three anonymous reviewers helped to improve the manuscript. Open Access funding enabled and organized by Projekt DEAL.

## DATA AVAILABILITY STATEMENT

The data that support the findings of this study are available from the corresponding author upon reasonable request.

## ORCID

*Max Wisshak* https://orcid.org/0000-0001-7531-3317
*Jörn Peckmann* https://orcid.org/0000-0002-8572-0060

## REFERENCES

Aloisi, G., Catherine, P., Rouchy, J.-M., Foucher, J.-P., & Woodside, J. (2000). Methane-related authigenic carbonates of Eastern Mediterranean Sea mud volcanoes and their possible relation to gas hydrate destabilisation. *Earth and Planetary Science Letters*, *184*, 321–338. https://doi.org/10.1016/S0012-821X(00)00322-8

Baumann, L., Birgel, D., Wagreich, M., & Peckmann, J. (2016). Microbially-driven formation of Cenozoic siderite and calcite concretions from eastern Austria. *Austrian Journal of Earth Sciences*, *109*, 211–232. https://doi.org/10.17738/ajes.2016.0016

Birgel, D., Feng, D., Roberts, H. H., & Peckmann, J. (2011). Changing redox conditions at cold seeps as revealed by authigenic carbonates from Alaminos Canyon, northern Gulf of Mexico. *Chemical Geology*, *285*, 82–96. https://doi.org/10.1016/j.chemgeo.2011.03.004

Birgel, D., & Peckmann, J. (2008). Aerobic methanotrophy at ancient marine methane seeps: A synthesis. *Organic Geochemistry*, *39*, 1659–1667. https://doi.org/10.1016/j.orggeochem.2008.01.023

Birgel, D., Peckmann, J., Klautzsch, S., Thiel, V., & Reitner, J. (2006). Anaerobic and aerobic oxidation of methane at Late Cretaceous seeps in the Western Interior Seaway, USA. *Geomicrobiology Journal*, *23*, 565–577. https://doi.org/10.1080/01490450600897369

Birgel, D., Thiel, V., Hinrichs, K.-U., Elvert, M., Campbell, K. A., Reitner, J., Farmer, J. D., & Peckmann, J. (2006). Lipid biomarker patterns of methane-seep microbialites from the Mesozoic convergent margin of California. *Organic Geochemistry*, *37*, 1289–1302. https://doi.org/10.1016/j.orggeochem.2006.02.004

Boetius, A., Ravenschlag, K., Schubert, C. J., Rickert, D., Widdel, F., Gieseke, A., Amann, R., Jørgensen, B. B., Witte, U., & Pfannkuche, O. (2000). A marine microbial consortium apparently mediating anaerobic oxidation of methane. *Nature*, *407*, 623–626. https://doi.org/10.1038/35036572

Boetius, A., & Wenzhöfer, F. (2013). Seafloor oxygen consumption fuelled by methane from cold seeps. *Nature Geoscience*, *6*, 725–734. https://doi.org/10.1038/ngeo1926

Bohrmann, G., Greinert, J., Suess, E., & Torres, M. (1998). Authigenic carbonates from the Cascadia subduction zone and their relation to gas hydrate stability. *Geology*, *26*, 647–650. https://doi.org/10.1130/0091-7613(1998)026<0647:ACFTCS>2.3.CO;2

Bohrmann, G., & Torres, M. E. (2006). Gas hydrates in marine sediments. In H. D. Schulz & M. Zabel (Eds.), *Marine Geochemistry* (pp. 481–512). Springer. https://link.springer.com/chapter/10.1007%2F3-540-32144-6_14

Bouloubassi, I., Nabais, E., Pancost, R. D., Lorre, A., & Taphanel, M. H. (2009). First biomarker evidence for methane oxidation at cold seeps in the Southeast Atlantic (REGAB pockmark). *Deep-Sea Research Part II-Topical Studies in Oceanography*, *56*, 2239–2247. https://doi.org/10.1016/j.dsr2.2009.04.006

Bouvier, P., Rohmer, M., Benveniste, P., & Ourisson, G. (1976). Δ8(14)-steroids in the bacterium *Methylococcus capsulatus*. *Biochemical Journal*, *159*, 267–271. https://doi.org/10.1042/bj1590267

Bowman, J. (2006). The Methanotrophs – The Families Methylococcaceae and Methylocystaceae. In M. Dworkin, S. Falkow, E. Rosenberg, K.-H. Schleifer, & E. Stackebrandt (Eds.), *The Prokaryotes* (Vol. *5*, pp. 266–289). Springer.

Cai, W.-J., Chen, F., Powell, E. N., Walker, S. E., Parsons-Hubbard, K. M., Staff, G. M, Wang, Y., Ashton-Alcox, K. A., Callender, W. R., & Brett, C. E. (2006). Preferential dissolution of carbonate shells driven by petroleum seep activity in the Gulf of Mexico. *Earth and Planetary Science Letters*, *248*, 227–243. https://doi.org/10.1016/j.epsl.2006.05.020

Campbell, K. A. (2006). Hydrocarbon seep and hydrothermal vent paleoenvironments and paleontology: Past developments and future research directions. *Palaeogeography, Palaeoclimatology, Palaeoecology*, *232*, 362–407. https://doi.org/10.1016/j.palaeo.2005.06.018

Campbell, K. A., Farmer, J. D., & Des Marais, D. (2002). Ancient hydrocarbon seeps from the Mesozoic convergent margin of California: carbonate geochemistry, fluids and palaeoenvironments. *Geofluids*, *2*, 63–94. https://doi.org/10.1046/j.1468-8123.2002.00022.x

Charlou, J. L., Donval, J. P., Fouquet, Y., Ondreas, H., Knoery, J., Cochonat, P., Levaché, D., Poirier, Y., Jean-Baptiste, P., Fourré, E., & Chazallon, B. (2004). Physical and chemical characterization of

gas hydrates and associated methane plumes in the Congo–Angola Basin. *Chemical Geology*, *205*, 405–425. https://doi.org/10.1016/j.chemgeo.2003.12.033

Coleman, M. L. (1993). Microbial processes: Controls on the shape and composition of carbonate concretions. *Marine Geology*, *113*, 127–140. https://doi.org/10.1016/0025-3227(93)90154-N

Collister, J., Summons, R. E., Lichtfouse, E., & Hayes, J. (1993). An isotopic biogeochemical study of the Green River oil shale. *Organic Geochemistry*, *19*, 265–276. https://www.sciencedirect.com/science/article/abs/pii/014663809290042V

Cordova-Gonzalez, A., Birgel, D., Kappler, A., & Peckmann, J. (2020). Carbon stable isotope patterns of cyclic terpenoids: A comparison of cultured alkaliphilic aerobic methanotrophic bacteria and methane-seep environments. *Organic Geochemistry*, *139*, 103940. https://doi.org/10.1016/j.orggeochem.2019.103940

Crémière, A., Pierre, C., Blanc-Valleron, M.-M., Zitter, T., Çağatay, M. N., & Henry, P. (2012). Methane-derived authigenic carbonates along the North Anatolian fault system in the Sea of Marmara (Turkey). *Deep-Sea Research Part I: Oceanographic Research Papers*, *66*, 114–130. https://doi.org/10.1016/j.dsr.2012.03.014

Dupraz, C., Reid, R. P., Braissant, O., Decho, A. W., Norman, R. S., & Visscher, P. T. (2009). Processes of carbonate precipitation in modern microbial mats. *Earth-Science Reviews*, *96*, 141–162. https://doi.org/10.1016/j.earscirev.2008.10.005

Durisch-Kaiser, E., Klauser, L., Wehrli, B., & Schubert, C. (2005). Evidence of intense archaeal and bacterial methanotrophic activity in the Black Sea water column. *Applied and Environmental Microbiology*, *71*, 8099–8106. https://doi.org/10.1128/AEM.71.12.8099-8106.2005

Elvert, M., & Niemann, H. (2008). Occurrence of unusual steroids and hopanoids derived from aerobic methanotrophs at an active marine mud volcano. *Organic Geochemistry*, *39*, 167–177. https://doi.org/10.1016/j.orggeochem.2007.11.006

Elvert, M., Suess, E., & Whiticar, M. (1999). Anaerobic methane oxidation associated with marine gas hydrates: Superlight C-isotopes from saturated and unsaturated $C_{20}$ and $C_{25}$ irregular isoprenoids. *Naturwissenschaften*, *86*, 295–300. https://doi.org/10.1007/s001140050619

Gallagher, K. L., Dupraz, C., & Visscher, P. T. (2014). Two opposing effects of sulfate reduction on carbonate precipitation in normal marine, hypersaline, and alkaline environments: COMMENT. *Geology*, *42*, e313–e314. https://doi.org/10.1130/G34639C.1

Garcia-Pichel, F. (2006). Plausible mechanisms for the boring on carbonates by microbial phototrophs. *Sedimentary Geology*, *185*, 205–213. https://doi.org/10.1016/j.sedgeo.2005.12.013

Garcia-Pichel, F., Ramírez-Reinat, E., & Gao, Q. (2010). Microbial excavation of solid carbonates powered by P-type ATPase-mediated transcellular $Ca^{2+}$ transport. *Proceedings of the National Academy of Sciences of the United States of America*, *107*, 21749–21754. https://doi.org/10.1073/pnas.1011884108

Golubic, S., Radtke, G., & Campion-Alsumard, T. L. (2005). Endolithic fungi in marine ecosystems. *Trends in Microbiology*, *13*, 229–235. https://doi.org/10.1016/j.tim.2005.03.007

Greinert, J., Bohrmann, G., & Suess, E. (2013). Gas hydrate-associated carbonates and methane-venting at Hydrate Ridge: Classification, distribution, and origin of authigenic lithologies. *Geophysical Monograph Series*, *124*, 99. https://doi.org/10.1029/GM124p0099

Guan, H., Birgel, D., Feng, D., Peckmann, J., Liu, L., Liu, L., & Tao, J. (2021). Lipids and their $\delta^{13}C$ values reveal carbon assimilation and cycling in the methane-seep tubeworm *Paraescarpia echinospica* from the South China Sea. *Deep-Sea Research Part I: Oceanographic Research Papers*, *174*, 103556. https://doi.org/10.1016/j.dsr.2021.103556

Hanson, R. S., & Hanson, T. E. (1996). Methanotrophic bacteria. *Microbiological Reviews*, *60*, 439–471. https://doi.org/10.1128/mr.60.2.439-471.1996

Himmler, T., Birgel, D., Bayon, G., Pape, T., Ge, L., Bohrmann, G., & Peckmann, J. (2015). Formation of seep carbonates along the Makran convergent margin, northern Arabian Sea and a molecular and isotopic approach to constrain the carbon isotopic composition of parent methane. *Chemical Geology*, *415*, 102–117. https://doi.org/10.1016/j.chemgeo.2015.09.016

Himmler, T., Brinkmann, F., Bohrmann, G., & Peckmann, J. (2011). Corrosion patterns of seep-carbonates from the eastern Mediterranean Sea. *Terra Nova*, *23*, 206–212. https://doi.org/10.1111/j.1365-3121.2011.01000.x

Jahnke, L. L., Summons, R. E., Hope, J. M., & des Marais, D. J. (1999). Carbon isotopic fractionation in lipids from methanotrophic bacteria II: The effects of physiology and environmental parameters on the biosynthesis and isotopic signatures of biomarkers. *Geochimica et Cosmochimica Acta*, *63*, 79–93. https://doi.org/10.1016/S0016-7037(98)00270-1

Juretschko, S., Timmermann, G., Schmid, M., Schleifer, K.-H., Pommerening-Röser, A., Koops, H.-P., & Wagner, M. (1998). Combined molecular and conventional analyses of nitrifying bacterium diversity in activated sludge: *Nitrosococcus mobilis* and *Nitrospira*-like bacteria as dominant populations. *Applied and Environmental Microbiology*, *64*, 3042–3051. https://doi.org/10.1128/AEM.64.8.3042-3051.1998

Kellermann, M. Y., Schubotz, F., Elvert, M., Lipp, J. S., Birgel, D., Prieto-Mollar, X., Dubilier, N., & Hinrichs, K.-U. (2012). Symbiont-host relationships in chemosynthetic mussels: a comprehensive lipid biomarker study. *Organic Geochemistry*, *43*, 112–124. https://doi.org/10.1016/j.orggeochem.2011.10.005

Kennett, J. P., Cannariato, K., Hendy, I., & Behl, R. (2003). *Methane Hydrates in Quaternary Climate Change: The Clathrate Gun Hypothesis* (1st ed.). American Geophysical Union. https://doi.org/10.1029/054SP

Knief, C. (2015). Diversity and habitat preferences of cultivated and uncultivated aerobic methanotrophic bacteria evaluated based on pmoA as molecular marker. *Frontiers in Microbiology*, *6*, 1346. https://doi.org/10.3389/fmicb.2015.01346

Krause, S., Aloisi, G., Engel, A., Liebetrau, V., & Treude, T. (2014). Enhanced calcite dissolution in the presence of the aerobic methanotroph *Methylosinus trichosporium*. *Geomicrobiology Journal*, *31*, 325–337. https://doi.org/10.1080/01490451.2013.834007

Lane, D. J. (1991). 16S/23S rRNA Sequencing. In E. Stackebrandt & M. Goodfellow (Eds.), *Nucleic Acid Techniques in Bacterial Systematic* (pp. 115–175). John Wiley and Sons.

Lanzén, A., Jørgensen, S. L., Huson, D. H., Gorfer, M., Grindhaug, S. H., Jonassen, I., Øvreås, L., & Urich, T. (2012). CREST – Classification resources for environmental sequence tags. *PLoS One*, *7*, e49334. https://doi.org/10.1371/journal.pone.0049334

Leprich, D. J., Flood, B. E., Schroedl, P. R., Ricci, E., Marlow, J. J., Girguis, P. R., & Bailey, J. V. (2021). Sulfur bacteria promote dissolution of authigenic carbonates at marine methane seeps. *The ISME Journal*, *15*, 2043–2056. https://doi.org/10.1038/s41396-021-00903-3

Lösekann, T., Knittel, K., Nadalig, T., Fuchs, B., Niemann, H., Boetius, A., & Amann, R. (2007). Diversity and abundance of aerobic and anaerobic methane oxidizers at the Haakon Mosby Mud Volcano, Barents Sea. *Applied and Environmental Microbiology*, *73*, 3348–3362. https://doi.org/10.1128/Aem.00016-07

Marcon, Y., Ondréas, H., Sahling, H., Bohrmann, G., & Olu, K. (2014). Fluid flow regimes and growth of a giant pockmark. *Geology*, *42*, 63–66. https://pubs.geoscienceworld.org/gsa/geology/article-abstract/42/1/63/131351/Fluid-flow-regimes-and-growth-of-a-giant-pockmark?redirectedFrom=fulltext

Marcon, Y., Sahling, H., Allais, A.-G., Bohrmann, G., & Olu, K. (2014). Distribution and temporal variation of mega-fauna at the Regab pockmark (Northern Congo Fan), based on a comparison of videomosaics and geographic information systems analyses. *Marine Ecology*, *35*, 77–95. https://doi.org/10.1111/maec.12056

Matsumoto, R. (1990). Vuggy carbonate crust formed by hydrocarbon seepage on the continental shelf of Baffin Island, northeast Canada. *Geochemical Journal*, *24*, 143–158.

Mau, S., Tu, T.-H., Becker, M., dos Santos Ferreira, C., Chen, J.-N., Lin, L.-H., Wang, P.-L., Lin, S., & Bohrmann, G. (2020). Methane seeps and independent methane plumes in the South China Sea offshore Taiwan. *Frontiers in Marine Science*, *7*, 543. https://doi.org/10.3389/fmars.2020.00543

McCaffrey, M. A., Farrington, J. W., & Repeta, D. J. (1989). Geochemical implications of the lipid composition of *Thioploca* spp. from the Peru upwelling region—15°S. *Organic Geochemistry*, *14*, 61–68. https://doi.org/10.1016/0146-6380(89)90019-3

Meister, P. (2013). Two opposing effects of sulfate reduction on carbonate precipitation in normal marine, hypersaline, and alkaline environments. *Geology*, *41*, 499–502. https://doi.org/10.1130/G34185.1

Natalicchio, M., Peckmann, J., Birgel, D., & Kiel, S. (2015). Seep deposits from northern Istria, Croatia: a first glimpse into the Eocene seep fauna of the Tethys region. *Geological Magazine*, *152*, 444–459. https://doi.org/10.1017/S0016756814000466

Naviaux, J. D., Subhas, A. V., Rollins, N. E., Dong, S., Berelson, W. M., & Adkins, J. F. (2019). Temperature dependence of calcite dissolution kinetics in seawater. *Geochimica et Cosmochimica Acta*, *246*, 363–384. https://doi.org/10.1016/j.gca.2018.11.037

Nichols, P. D., Guckert, J. B., & White, D. C. (1986). Determination of monosaturated fatty acid double-bond position and geometry for microbial monocultures and complex consortia by capillary GC-MS of their dimethyl disulphide adducts. *Journal of Microbiological Methods*, *5*, 49–55. https://doi.org/10.1016/0167-7012(86)90023-0

Niemann, H., Elvert, M., Hovland, M., Orcutt, B., Judd, A., Suck, I., Gutt, J., Joye, S., Damm, E., Finster, K., & Boetius, A. (2005). Methane emissions and consumption at a North Sea gas seep (Tommeliten area). *Biogeosciences*, *2*, 335–351. https://doi.org/10.5194/bg-2-335-2005

Olu, K. (2011). WACS cruise, RV Pourquoi pas? https://doi.org/10.17600/11030010

Olu-Le Roy, K., Caprais, J.-C., Fifis, A., Fabri, M.-C., Galéron, J., Budzinsky, H., Le Ménach, K., Khripounoff, A., Ondréas, H., & Sibuet, M. (2007). Cold-seep assemblages on a giant pockmark off West Africa: spatial patterns and environmental control. *Marine Ecology*, *28*, 115–130. https://doi.org/10.1111/j.1439-0485.2006.00145.x

Ondréas, H., Olu, K., Fouquet, Y., Charlou, J. L., Gay, A., Dennielou, B., Donval, J. P., Fifis, A., Nadalig, T., Cochonat, P., Cauquil, E., Bourillet, J. F., Moigne, M. L., & Sibuet, M. (2005). ROV study of a giant pockmark on the Gabon continental margin. *Geo-Marine Letters*, *25*, 281–292. https://doi.org/10.1007/s00367-005-0213-6

Ourisson, G., Albrecht, P., & Rohmer, M. (1979). The hopanoids. Palaeochemistry and biochemistry of a group of natural products. *Pure and Applied Chemistry*, *51*, 709–729. https://doi.org/10.1351/pac197951040709

Ourisson, G., Rohmer, M., & Poralla, K. (1987). Prokaryotic hopanoids and other polyterpenoid sterol surrogates. *Annual Review of Microbiology*, *41*, 301–333. https://doi.org/10.1146/annurev.mi.41.100187.001505

Parks, D. H., Chuvochina, M., Waite, D. W., Rinke, C., Skarshewski, A., Chaumeil, P.-A., & Hugenholtz, P. (2018). A standardized bacterial taxonomy based on genome phylogeny substantially revises the tree of life. *Nature Biotechnology*, *36*, 996–1004. https://doi.org/10.1038/nbt.4229

Peckmann, J., Reimer, A., Luth, U., Luth, C., Hansen, B. T., Heinicke, C., Hoefs, J., & Reitner, J. (2001). Methane-derived carbonates and authigenic pyrite from the northwestern Black Sea. *Marine Geology*, *177*, 129–150. https://doi.org/10.1016/S0025-3227(01)00128-1

Peckmann, J., & Thiel, V. (2004). Carbon cycling at ancient methane-seeps. *Chemical Geology*, *205*, 443–467. https://doi.org/10.1016/j.chemgeo.2003.12.025

Pierre, C., & Fouquet, Y. (2007). Authigenic carbonates from methane seeps of the Congo deep-sea fan. *Geo-Marine Letters*, *27*, 249–257. https://doi.org/10.1007/s00367-007-0081-3

Pond, D. W., Bell, M. V., Dixon, D. R., Fallick, A. E., Segonzac, M., & Sargent, J. R. (1998). Stable-carbon-isotope composition of fatty acids in hydrothermal vent mussels containing methanotrophic and thiotrophic bacterial endosymbionts. *Applied and Environmental Microbiology*, *64*, 370–375. https://doi.org/10.1128/AEM.64.1.370-375.1998

Pop Ristova, P., Wenzhöfer, F., Ramette, A., Zabel, M., Fischer, D., Kasten, S., & Boetius, A. (2012). Bacterial diversity and biogeochemistry of different chemosynthetic habitats of the REGAB cold seep (West African margin, 3160 m water depth). *Biogeosciences*, *9*, 5031–5048. https://doi.org/10.5194/bg-9-5031-2012

Radtke, G. (1991). Die mikroendolithischen Spurenfossilien im Alt-Tertiär West-Europas und ihre palökologische Bedeutung. In *Courier Forschungsinstitut Senckenberg* (Vol. *138*, pp. 1–150). Schweizerbart Science Publishers. https://www.schweizerbart.de//publications/detail/isbn/9783510611294/CFS_Courier_Forschungsinstitut_Senckenbe

Radtke, G., Glaub, I., Vogel, K., & Golubic, S. (2010). A new dichotomous microboring: *Abeliella bellafurca* isp. nov., distribution, variability and biological origin. *Ichnos*, *17*, 25–33. https://doi.org/10.1080/10420940903358628

Ruppel, C. D., & Kessler, J. D. (2016). The interaction of climate change and methane hydrates. *Reviews of Geophysics*, *55*, 126–168. https://doi.org/10.1002/2016RG000534

Rush, D., Osborne, K. A., Birgel, D., Kappler, A., Hirayama, H., Peckmann, J., Poulton, S. W., Nickel, J. C., Mangelsdorf, K., Kaluzhnaya, M., Sidgwick, F. R., & Talbot, H. M. (2016). The bacteriohopanepolyol inventory of novel aerobic methane oxidising bacteria reveals new biomarker signatures of aerobic methanotrophy in marine systems. *PLoS One*, *11*, e0165635. https://doi.org/10.1371/journal.pone.0165635

Sahling, H., Rickert, D., Lee, W. L., Linke, P., & Suess, E. (2002). Macrofaunal community structure and sulfide flux at gas hydrate deposits from the Cascadia convergent margin, NE Pacific. *Marine Ecology Progress Series*, *231*, 121–138. https://doi.org/10.3354/meps231121

Sandy, M. R., Lazar, I., Peckmann, J., Birgel, D., Stoica, M., & Roban, R. D. (2012). Methane-seep brachiopod fauna within turbidites of the Sinaia Formation, Eastern Carpathian Mountains, Romania. *Palaeogeography Palaeoclimatology Palaeoecology*, *323*, 42–59. https://doi.org/10.1016/j.palaeo.2012.01.026

Schouten, S., Bowman, J. P., Rijpstra, W. I., & Sinninghe Damsté, J. S. (2000). Sterols in a psychrophilic methanotroph, *Methylosphaera hansonii*. *FEMS Microbiology Letters*, *186*, 193–195.

Sloan, E. D. (2003). Fundamental principles and applications of natural gas hydrates. *Nature*, *426*, 353–359. https://doi.org/10.1038/nature02135

Subhas, A. V., Adkins, J. F., Rollins, N. E., Naviaux, J., Erez, J., & Berelson, W. M. (2017). Catalysis and chemical mechanisms of calcite dissolution in seawater. *Proceedings of the National Academy of Sciences of the United States of America*, *114*, 8175–8180. https://doi.org/10.1073/pnas.1703604114

Suess, E. (2014). Marine cold seeps and their manifestations: geological control, biogeochemical criteria and environmental conditions. *International Journal of Earth Sciences*, *103*, 1889–1916. https://doi.org/10.1007/s00531-014-1010-0

Suess, E., Torres, M. E., Bohrmann, G., Collier, R. W., Greinert, J., Linke, P., Rehder, G., Trehu, A., Wallmann, K., Winckler, G., & Zuleger, E. (1999). Gas hydrate destabilization: enhanced dewatering, benthic material turnover and large methane plumes at the Cascadia convergent margin. *Earth and Planetary Science Letters*, *170*, 1–15. https://doi.org/10.1016/S0012-821X(99)00092-8

Summons, R. E., Bradley, A. S., Jahnke, L. L., & Waldbauer, J. R. (2006). Steroids, triterpenoids and molecular oxygen. *Philosophical*

*Transactions of the Royal Society B Biological Sciences*, *361*, 951–968. https://doi.org/10.1098/rstb.2006.1837

Talbot, H. M., Handley, L., Spencer-Jones, C. L., Dinga, B. J., Schefuß, E., Mann, P. J., Poulsen, J. R., Spencer, R. G. M., Wabakanghanzi, J. N., & Wagner, T. (2014). Variability in aerobic methane oxidation over the past 1.2 Myrs recorded in microbial biomarker signatures from Congo fan sediments. *Geochimica et Cosmochimica Acta*, *133*, 387–401. https://www.sciencedirect.com/science/article/pii/S0016703714001446

Talbot, H. M., Watson, D. F., Murrell, J. C., Carter, J. F., & Farrimond, P. (2001). Analysis of intact bacteriohopanepolyols from methanotrophic bacteria by reversed-phase high-performance liquid chromatography-atmospheric pressure chemical ionisation mass spectrometry. *Journal of Chromatography A*, *921*, 175–185. https://doi.org/10.1016/S0021-9673(01)00871-8

Urich, T., Lanzén, A., Qi, J., Huson, D. H., Schleper, C., & Schuster, S. C. (2008). Simultaneous assessment of soil microbial community structure and function through analysis of the meta-transcriptome. *PLoS One*, *3*, e2527. https://doi.org/10.1371/journal.pone.0002527

Wei, J. H., Yin, X. C., & Welander, P. V. (2016). Sterol synthesis in diverse bacteria. *Frontiers in Microbiology*, *7*, 990. https://doi.org/10.3389/fmicb.2016.00990

Willers, C., Jansen van Rensburg, P. J., & Claassens, S. (2015). Phospholipid fatty acid profiling of microbial communities–a review of interpretations and recent applications. *Journal of Applied Microbiology*, *119*, 1207–1218. https://doi.org/10.1111/jam.12902

Wisshak, M. (2012). Microbioerosion. In D. Knaust & R. G. Bromley (Eds.), *Trace Fossils as Indicators of Sedimentary Environments*. *Developments in Sedimentology* (Vol. *64*, pp. 213–243). Elsevier. https://doi.org/10.1016/B978-0-444-53813-0.00008-3

Wisshak, M., Knaust, D., & Bertling, M. (2019). Bioerosion ichnotaxa: review and annotated list. *Facies*, *65*, 24. https://doi.org/10.1007/s10347-019-0561-8

Wisshak, M., Tribollet, A., Jakobsen, J., & Freiwald, A. (2011). Temperate bioerosion: Ichnodiversity and biodiversity from intertidal to bathyal depths (Azores). *Geobiology*, *9*, 492–520. https://doi.org/10.1111/j.1472-4669.2011.00299.x

Woosley, R. J. (2016). Carbonate Compensation Depth. In W. M. White (Ed.), *Encyclopedia of Geochemistry. Encyclopedia of Earth Sciences Series* (pp. 204–205). Springer. https://doi.org/10.1007/978-3-319-39312-4_85

Xie, S., Lipp, J. S., Wegener, G., Ferdelman, T. G., & Hinrichs, K.-U. (2013). Turnover of microbial lipids in the deep biosphere and growth of benthic archaeal populations. *Proceedings of the National Academy of Sciences of the United States of America*, *110*, 6010–6014. https://doi.org/10.1073/pnas.1218569110

Zabel, M., Boetius, A., Emeis, K.-C., Ferdelman, T. G., & Spieß, V. (2012). *PROSA Process Studies in the Eastern South Atlantic – Cruise No.* M76 – April 12 – August 24, 2008 – Cape Town (South Africa) – Walvis Bay (Namibia) Meteor R/V. DFG-Senatskommission für Ozeanographie. https://doi.org/10.2312/cr_m76

## SUPPORTING INFORMATION

Additional supporting information can be found online in the Supporting Information section at the end of this article.

**How to cite this article:** Cordova-Gonzalez, A., Birgel, D., Wisshak, M., Urich, T., Brinkmann, F., Marcon, Y., Bohrmann, G., & Peckmann, J. (2023). A carbonate corrosion experiment at a marine methane seep: The role of aerobic methanotrophic bacteria. *Geobiology*, *21*, 491–506. https://doi.org/10.1111/gbi.12549